DOI: 10.61782/fa.2025.0537

FORUM ACUSTICUM
EURONOISE 2025

LOW-NOISE PROPELLER OPTIMIZATION VIA BLADE SWEEP AND UNEVEN SPACING

Felice Fruncillo[1,2*] **Paolo Luchini**[1] **Flavio Giannetti**[1]

[1] University of Salerno, Via Giovanni Paolo II, 132, Fisciano, 84084, Italy
[2] Italian Aerospace Research Center, Via Maiorise, Capua, 81043, Italy

ABSTRACT

The present study investigates the impact of propeller planform on noise emission. Both balanced and unbalanced configurations are considered, acting on blade spacing and sweep. A global optimization, where the objective function is the sound pressure in the plane of rotation, confirms that uneven blade spacing can reduce noise. However, this does not necessarily lead to a reduction in emitted power. It is indeed the case that a stronger radiation in other directions results in an increase in the total noise from the source. Conversely, sweep optimization yields greater benefits, ensuring both local and overall noise reduction. An analysis of unbalanced rotors provides slightly improved results, but not enough to justify such a design.

Keywords: *Uneven spacing, blade sweep, balanced rotor, multipole expansion.*

1. INTRODUCTION

Significant progress has been made in the study of rotor noise, with a focus on mitigating the acoustic emissions of propeller systems. Various approaches have been explored to understand how different configurations influence noise generation in both unmanned aerial vehicles (UAVs) and conventional aircraft. Key strategies include geometrical modifications, integration of porous materials, edge serrations, boundary layer tripping mechanisms, and synchrophasing techniques [1–4]. To achieve optimal noise reduction, a multidisciplinary optimization framework is often necessary, considering together aerodynamics, acoustics, and structural integrity [5]. This ensures that propeller performance or mechanical strength is not compromised when acoustic requirements are followed [6]. Studies highlight that propeller configuration plays a crucial role in shaping the acoustic characteristics of radiated noise, reinforcing the importance of blade geometry in its reduction.

In this paper, the effects of unequal blade spacing and sweep on propeller noise are the primary focus. Dobrzynski's seminal research [7] has demonstrated that appropriately adjusting the blade spacing in the circumferential direction can effectively reduce tonal noise in the plane of rotation. This is true over a broad range of tip Mach numbers (M_t). Conventional propellers typically employ equally spaced blades to maintain aerodynamic balance and performance; this uniform spacing concentrates noise at distinct frequencies (Blade Passing Frequencies, BPF), making it more perceptible. Uneven blade spacing, where blades are deliberately positioned at unequal intervals, can redistribute noise energy in the frequency spectrum, thereby reducing the amplitude of dominant noise peaks. Experimental analyses too indicate that noise reductions up to 4 dBA can be achieved, compared to even configurations, particularly at high subsonic tip Mach numbers [8]. Notably, these reductions are achieved without compromising aerodynamic performance, establishing it as a promising noise mitigation strategy. However, psychoacoustic evaluations have not consistently confirmed these advantages, since subjective assessments of loudness in-

*Corresponding author: ffruncillo@unisa.it.

dicate minimal perceptual differences between propellers with and without uniform blade spacing [9].

The objective of this study is to build upon the research conducted by Dobrzynski. In particular, an examination of both balanced and unbalanced rotor configurations is made, in order to determine their effectiveness in reducing noise within the rotational plane. The assumption of identical blades is removed, and the effect of blade sweep is considered into the optimization process. Moreover, a multipole expansion approach is employed to assess the total emitted power. This allows for the evaluation of whether the noise reduction benefits observed in the rotational plane are indicative of a decrease in the overall noise emitted by the source. Only when this occurs can it be confirmed that a quieter propeller has been achieved.

2. MULTIPOLE FORMULATION

In a recent paper, still under review, these authors proposed a multipole expansion approach for the prediction of the acoustic field generated by rotating blades in hovering. A preliminary version is available in [10]. The hypothesis underlying the model concerns the possibility of reducing the rotor to a planar surface, thus being valid for blades that are not too twisted and at low incidence. Under these assumptions, the two components of thickness and loading noise are obtained by exploiting the results of thin airfoil theory. Among the assumptions is that of equal and equally spaced blades.

The formulation remains largely valid in the case of uneven spacing. The main change concerns the azimuthal Fourier coefficients. Indeed, the frequency domain formulation is achieved by performing a Fourier transform in time of the Green integral equation, assuming periodic boundary conditions in the local blade coordinate ϕ'. Considering the pressure coefficient jump $\Delta\bar{c}_p$ with unitary integrated value, and the thickness function H scaled with chord length, as function of ϕ' and spanwise coordinate $\bar{r}$, it results

$$\Delta\bar{c}_p\left(\bar{r},\phi'\right) = \sum_{m=-\infty}^{\infty} \Delta\bar{c}_{p_m}\left(\bar{r}\right) e^{im\phi'} \tag{1}$$

$$H\left(\bar{r},\phi'\right) = \sum_{m=-\infty}^{\infty} H_m\left(\bar{r}\right) e^{im\phi'} \tag{2}$$

where $\bar{r}$ varies from $\bar{R}_{hub} = \frac{R_{hub}}{R}$ to 1, with R_{hub} and R denoting the hub and tip blade lengths, respectively. In the case of N equally spaced blades, the period is $\frac{2\pi}{N}$ and non-zero Fourier coefficients are those for which m is a multiple, both positive and negative, of N. In a more general case, looking only at thickness as example, one must consider

$$H_m\left(\bar{r}\right) = \frac{1}{2\pi}\int_0^{2\pi} H\left(\bar{r},\phi'\right) e^{-im\phi'} d\phi' \tag{3}$$

In the case where, starting with the first blade, the others are arranged at angles α_b and exactly identical to each other, the Fourier coefficients are obtained as

$$H_m\left(\bar{r}\right) = \frac{1}{2\pi}\int_{\phi'_{TE}(\bar{r})}^{\phi'_{LE}(\bar{r})} H\left(\bar{r},\phi'\right) e^{-im\phi'} d\phi' \sum_{b=0}^{N-1} e^{-im\alpha_b} \tag{4}$$

where ϕ'_{LE} and ϕ'_{TE} represent the planform of leading and trailing edges, thus defining the sweep of the blade. In the case of N blades placed at angles $\alpha_b = 2\pi b/N$, the sum in Eqn. (4) would reduce to a geometric series, which equals N when m is a multiple of N, and zero in all other cases, i.e. retrieving the particular case of even spacing. In this way, loading and thickness noise formulae can still be applied in the unequally spaced case, with the understanding that all harmonics m and the factor derived from the geometric series must be taken into account. Multipole coefficients for loading noise turn out to be

$$A_{L_{lm}} = i\rho a_s^2 M_t^3 m B_{L_{lm}} \sum_{b=0}^{N-1} e^{-im\alpha_b} \int_{\bar{R}_{hub}}^{1} j_l\left(mM_t\bar{r}\right)\gamma c_l \Delta\bar{c}_{p_m}\bar{r}e^{-im\phi'_{TE}} d\bar{r} \tag{5}$$

and for thickness noise

$$A_{T_{lm}} = -4i\rho a_s^2 M_t^3 m^3 B_{T_{lm}} \sum_{b=0}^{N-1} e^{-im\alpha_b} \int_{\bar{R}_{hub}}^{1} j_l\left(mM_t\bar{r}\right)\gamma^2 H_m e^{-im\phi'_{TE}} d\bar{r} \tag{6}$$

where j_l is the spherical Bessel function of order l, γ is the chord-to-diameter ratio, ρ and a_s are air density and speed of sound, $B_{L_{lm}}$ and $B_{T_{lm}}$ are constants depending on m and l values.

The solution of the wave equation in the domain outside the sphere containing the sources can be obtained by the multipole expansions for loading and thickness com-

ponents, respectively given by [11]

$$p_{L_m}(\mathbf{x}_0) = \sum_{\substack{l=|m| \\ l-m \text{ odd}}}^{\infty} A_{L_{lm}} h_l(mM_t\bar{r}_0) Y_{lm}(\theta_0, \phi_0) \quad (7)$$

$$p_{T_m}(\mathbf{x}_0) = \sum_{\substack{l=|m| \\ l-m \text{ even}}}^{\infty} A_{T_{lm}} h_l(mM_t\bar{r}_0) Y_{lm}(\theta_0, \phi_0) \quad (8)$$

where h_l is the spherical Hankel function (of the first kind) of order l, Y_{lm} are the spherical harmonics and subscript 0 is used to indicate observer position in spherical coordinates ($r_0 = \bar{r}_0 R$, θ_0 and ϕ_0). Radiated powers are obtained straightforwardly from [12]

$$\Pi_{L_m} = \frac{R^2}{2\rho a_s M_t^2 m^2} \sum_{\substack{l=|m| \\ l-m \text{ odd}}}^{\infty} |A_{L_{lm}}|^2 \quad (9)$$

$$\Pi_{T_m} = \frac{R^2}{2\rho a_s M_t^2 m^2} \sum_{\substack{l=|m| \\ l-m \text{ even}}}^{\infty} |A_{T_{lm}}|^2 \quad (10)$$

3. OPTIMIZATION RESULTS

The objective of this section is to optimize the traditional 6-blade rotor configuration shown in Fig. 1. In this case, the blades are identical, unswept and equally spaced. The optimization is performed by minimising the noise emitted at a far-field point ($\bar{r}_0 = 100$) in the plane of rotation ($\theta_0 = 90°$). For the initial configuration, a spanwise chord distribution typical of drone blades [13] is considered. Chordwise pressure coefficient is obtained from XFOIL [14] and assumed to be the same for each spanwise station; thickness is related to a NACA 0012 airfoil. For tip Mach equal to $M_t = 0.8$, the obtained values of A-weighted overall sound pressure level (OSPL) and sound power level (OSWL) are 86.67 dBA and 111.89 dBA, respectively.

The optimized planform configurations examined in this study are divided into two categories: balanced and unbalanced rotors, each consisting of six blades numbered counter-clockwise from 0 to 5. A balanced rotor is characterised by having pair of opposite blades that are equal to each other, ensuring that the centre of mass remains at the centre of the rotor; in contrast, an unbalanced rotor does not have this constraint. For both types, three distinct configurations are considered. The first one optimizes the position in the plane of identical unswept

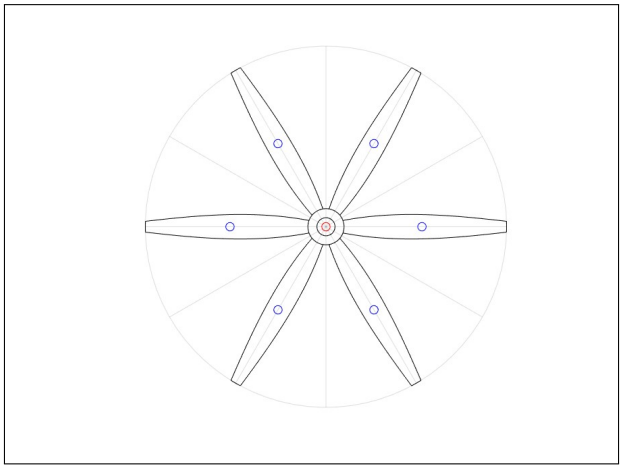

Figure 1. Reference rotor.

blades, acting on the values of α_b (α_0 is always considered to be zero). The second also considers homothetically scaled blades, by optimizing different weights w_b, such that $\gamma_b = w_b\gamma$, but ensuring unchanged rotor solidity ($\sum_b w_b = N$). The third configuration considers, in addition to the spacing in the plane, the optimization of the sweep. This is determined by the spanwise distribution of the function $\phi'_{TE}(\bar{r})$, which is obtained through cubic Bézier curves. Each of these curves is characterised by four control points, denoted by β_k, to be optimized. To prevent the overlap of adjacent blades, non-linear constraints are imposed and each blade is bound to occupy a maximum of 30 azimuthal degrees. The optimization uses a global search strategy to avoid local minima, which can affect the solution. To this end, the Matlab GlobalSearch function is employed in conjunction with fmincon. The six configurations are outlined in Tab. 1, which provides the number of parameters to be optimized in each case. In each scenario, the solver starts from the same initial guess condition, which coincides with the rotor in Fig. 1.

3.1 Balanced rotor

The first configuration (1-BAL) is the one studied by Dobrzynski. He found that the optimal solution involves having the blade number 1 equispaced by the two adjacent ones, i.e. such that the relation $\alpha_2 = 2\alpha_1$ holds. These values depend almost exclusively on the tip Mach and tend to decrease when it increases. In accordance with this, the optimal configuration found is given in Fig. 2. The position of the centre of gravity of each blade is indicated

Table 1. Rotor's configurations to be optimized.

Configuration	Parameters
1-BAL	2 α_b
2-BAL	2 α_b + 3 w_b
3-BAL	2 α_b + 12 β_k
1-UNBAL	5 α_b
2-UNBAL	5 α_b + 6 w_b
3-UNBAL	5 α_b + 24 β_k

by the blue circles, while the red one denotes the centre of gravity of the entire rotor. Given the relatively high M_t, optimization leads to $\alpha_1 \approx 40°$, which corresponds to the minimum possible value given by the size of the blades. Further analyses at decreasing tip Mach confirmed the trend discussed above. In this configuration, the noise at observer position is reduced by 0.45 dBA, compared to the reference. As far as power is concerned, however, it is 0.14 dBA higher. A reduction in the length of the chord yields qualitatively similar results, but the increase in pressure in the plane and the increase in power are more pronounced, since smaller α can be obtained. Specifically, considering half chord values, $\alpha_1 \approx 20°$ is obtained, with a pressure reduction of 2.13 dBA and a power increase of 3.40 dBA.

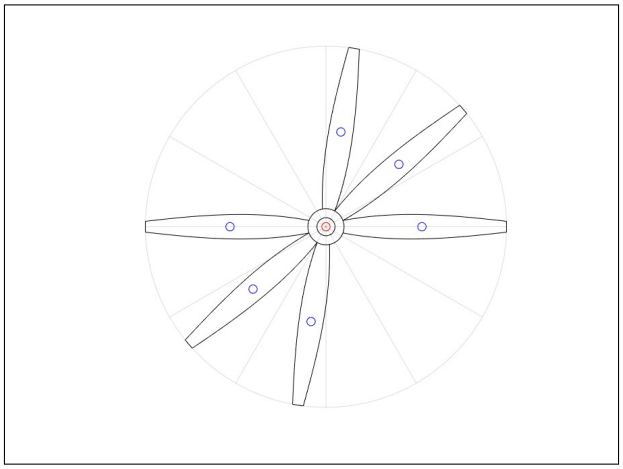

Figure 2. 1-BAL optimal configuration.

With regard to the 2-BAL configuration, this adds to the previous one the possibility of having different chords between the blades, while ensuring an unchanged solidity of the rotor. However, optimization has shown this to be an inefficient solution. The values obtained result in two blades with a chord increased by just 0.7% and the remaining four reduced by 0.35%. The values of the parameter α remain almost unchanged compared to the previous case, net of a slightly different footprint. Consequently, OSPL is reduced by only approximately three decimal digits compared to the first configuration. The rotor is not shown here, as it is indistinguishable from the previous one.

A more interesting solution is found in the 3-BAL configuration. In this case, in addition to the α values, the blade sweep is optimized, acting on ϕ'_{TE}. The optimal rotor is illustrated in Fig. 3. The blades exhibit a pronounced sweep opposite to the direction of rotation, resulting in substantial benefits in terms of noise emission. Indeed, the pressure in the plane is reduced by 9.48 dBA, and in this instance the power is also reduced by 4.01 dBA.

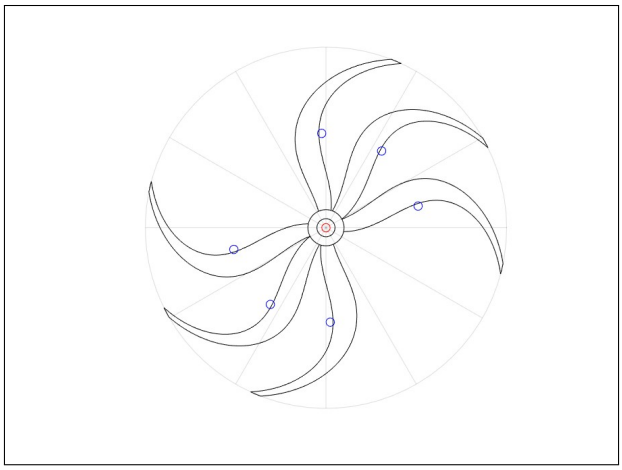

Figure 3. 3-BAL optimal configuration.

The resume of the three optimized balanced configurations can be found in Tab. 2.

Table 2. Optimization results for balanced configurations. Negative values indicate noise reduction.

Configuration	Δ SPL [dBA]	Δ SWL [dBA]
1-BAL	−0.45	0.14
2-BAL	−0.45	0.13
3-BAL	−9.48	−4.01

To understand the reasons for the different effect obtained on pressure and power, a plot of OSPL as a function of elevation angle θ_0 is shown in Fig. 4. It is evident that the optimized configurations, while reducing the pressure in the plane ($\theta_0 = 90°$), tend to increase it in other directions. This leads to the possibility of an increase in the total power emitted by the source. It is worth noting that when considering the plane of rotation, only the thickness component is non-zero, as the loading one is antisymmetric.

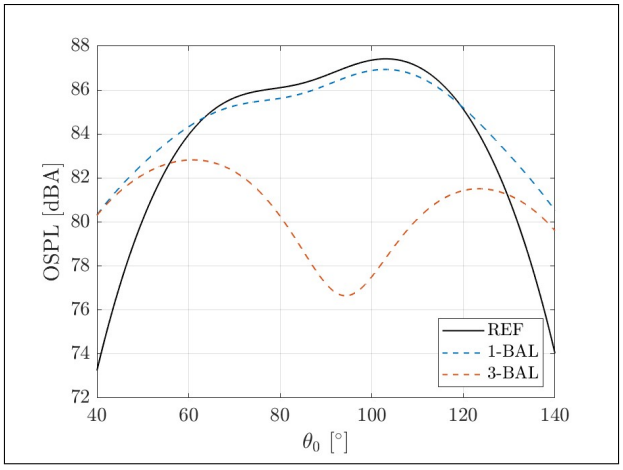

Figure 4. Polar radiation for balanced configurations.

The redistribution of noise in frequency can be appreciated in Fig. 5 and Fig. 6 for pressure and power, respectively. The initial configuration manifests peaks at the BPF (m multiples of N), with the typical decreasing trend in frequency; in the other cases, more tones appear as the source frequency is one third of the initial one, and the trend is strongly oscillating. In particular, it can be seen that in the optimized solutions it is not the first frequency that dominates the spectrum, but a higher one.

3.2 Unbalanced rotor

For unbalanced rotors, the constraint of having pairs of equal blades repeated every 180° is removed. The first configuration (1-UNBAL) therefore comprises five angles which must be optimized. The result is partly predictable: the blades tend to be all on one side, equispaced by the same $\alpha \approx 40°$ as the balanced configuration. The rotor is shown in Fig. 7, where the off-centre position of the centre of gravity can be seen. This solution is indeed better than

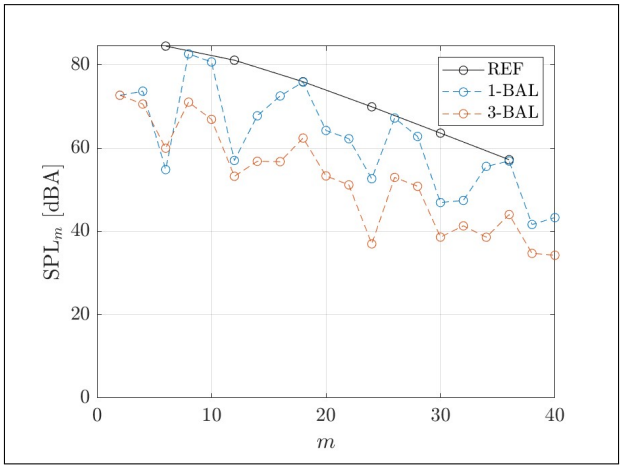

Figure 5. A-weighted SPL versus frequency, for balanced configurations.

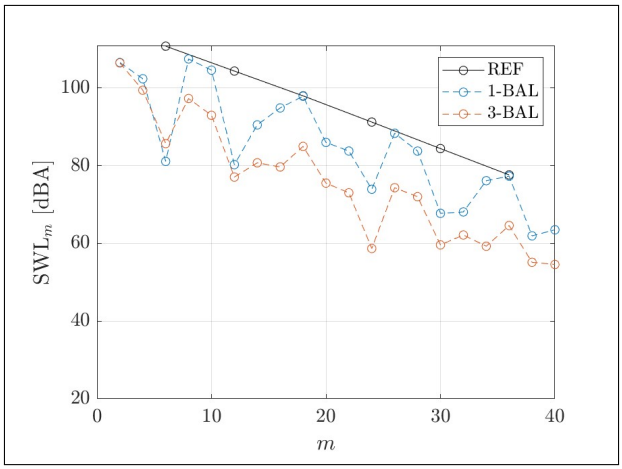

Figure 6. A-weighted SWL versus frequency, for balanced configurations.

the balanced one in reducing the in-plane noise, but the 0.62 dBA decrease would not justify such a choice. The half-chord analysis resulted in a pressure reduction of 3.86 dBA, but a power increase of 2.32 dBA.

Analogous considerations apply to the 2-UNBAL configuration as they do to the balanced case.

Conversely, the unbalanced swept rotor (3-UNBAL) leads to a local minimum solution shown in Fig. 8. The noise reduction is less than that of the 3-BAL configuration, but it is still significant (8.79 dBA) and is therefore reported. To prevent local minima, an optimization could

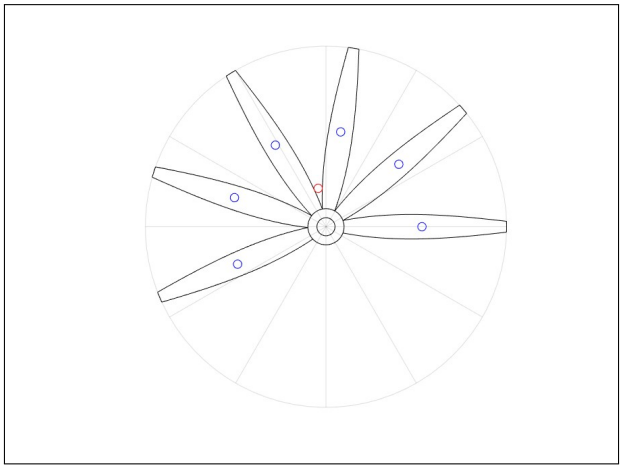

Figure 7. 1-UNBAL optimal configuration.

be made by considering the balanced configuration as an initial guess condition for the solver.

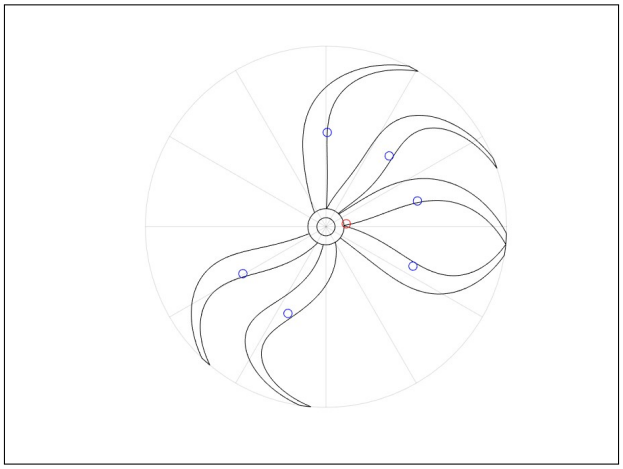

Figure 8. 3-UNBAL optimal configuration.

The resume of the three optimized configurations is reported in Tab. 3, while the polar radiation diagram is in Fig. 9. The frequency trends are illustrated in Fig. 10 and Fig. 11. In this instance, the initial non-zero harmonic is $m = 1$, since the sources repeat spatially every complete rotation.

Table 3. Optimization results for unbalanced configurations. Negative values indicate noise reduction.

Configuration	Δ SPL [dBA]	Δ SWL [dBA]
1-UNBAL	−0.62	−0.49
2-UNBAL	−0.62	−0.49
3-UNBAL	−8.79	−2.66

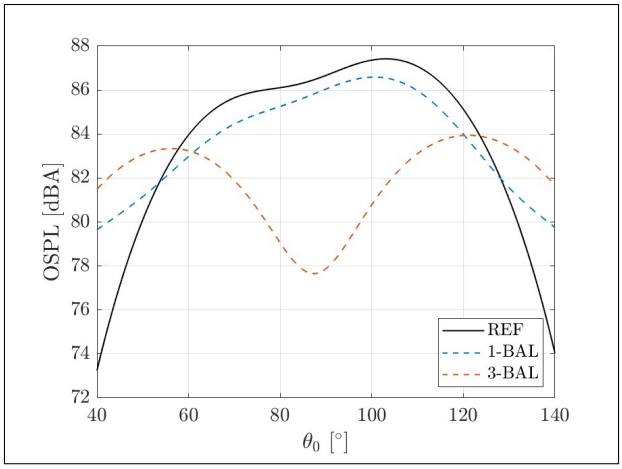

Figure 9. Polar radiation for unbalanced configurations.

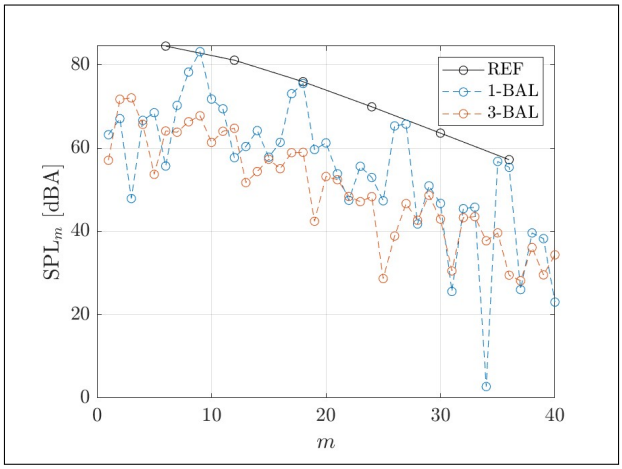

Figure 10. A-weighted SPL versus frequency, for unbalanced configurations.

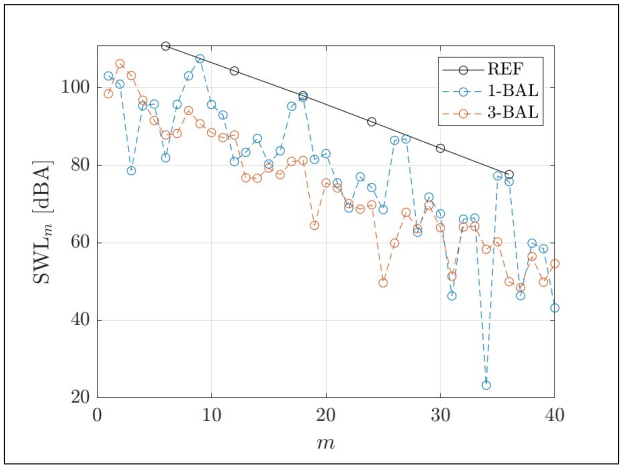

Figure 11. A-weighted SWL versus frequency, for unbalanced configurations.

4. CONCLUSIONS

The planform optimization of a 6-blade propeller has demonstrated the possibilities of reducing the noise emitted in the plane of rotation. It has been observed in the literature that unevenly spaced blades gives good results. However, the present study has shown that this does not necessarily lead to a reduction in the total power emitted by the source, which could more appropriately be taken as an objective function. The sweep effect yielded significant benefits and, in the considered configurations, it has ensured a reduction in power too. Conversely, the prospect of unbalanced rotors appears to be unpromising, as it would only lead to a modest reduction in dBA, whereas entailing technical problems of rebalancing.
Further analyses will be conducted to evaluate different objective functions and the effects of the other parameters involved in the optimization.

5. REFERENCES

[1] F. Avallone, W. van der Velden, D. Ragni, and D. Casalino, "Noise reduction mechanisms of sawtooth and combed-sawtooth trailing-edge serrations," *Journal of Fluid Mechanics*, vol. 848, pp. 560–591, 08 2018.

[2] P. Candeloro, D. Ragni, and T. Pagliaroli, "Small-scale rotor aeroacoustics for drone propulsion: a review of noise sources and control strategies," *Fluids*, vol. 7, no. 8, p. 279, 2022.

[3] M. Shao, Y. Lu, X. Xu, S. Guan, and J. Lu, "Experimental study on noise reduction of multi-rotor by phase synchronization," *Journal of Sound and Vibration*, vol. 539, p. 117199, 2022.

[4] F. Fruncillo, P. Luchini, F. Giannetti, R. Tognaccini, and M. Massa, "Propeller optimization for tonal noise reduction using spherical harmonics expansion and blade element theory," in *30th AIAA/CEAS Aeroacoustics Conference (2024)*, p. 3320, 2024.

[5] O. Gur and A. Rosen, "Multidisciplinary design optimization of a quiet propeller," in *14th AIAA/CEAS Aeroacoustics Conference (29th AIAA Aeroacoustics Conference)*, p. 3073, 2008.

[6] C. J. Miller and J. P. Sullivan, "Noise constraints effecting optimal propeller designs," *SAE transactions*, pp. 585–593, 1985.

[7] W. Dobrzynski, "Propeller noise reduction by means of unsymmetrical blade-spacing," *Journal of Sound and Vibration*, vol. 163, no. 1, pp. 123–126, 1993.

[8] T. Y. Kim, *Reduction of tonal propeller noise by means of uneven blade spacing*. University of California, Irvine, 2016.

[9] H. Fastl and I. Stemplinger, "Psychoacoustic evaluation of noises produced by propellers with asymmetrical blade spacing," in *41st International Congress and Exposition on Noise Control Engineering, INTER-NOISE, New York City, USA*, 2012.

[10] F. Fruncillo, P. Luchini, and F. Giannetti, "Multipole expansion approach for rotor noise prediction and optimization," *Available at SSRN 4929758*.

[11] J. Jackson, *Classical Electrodynamics*. Wiley, 2012.

[12] E. G. Williams and I. Mann, J. Adin, "Fourier Acoustics: Sound Radiation and Nearfield Acoustical Holography ," *The Journal of the Acoustical Society of America*, vol. 108, pp. 1373–1373, 10 2000.

[13] F. Fruncillo, L. Federico, M. Cicala, and R. Citarella, "Development and validation of an aeropropulsive and aeroacoustic simulation model of a quadcopter drone," *Drones*, vol. 6, no. 6, 2022.

[14] M. Drela, "Xfoil: An analysis and design system for low reynolds number airfoils," vol. 54, 06 1989.